Study of a Li–air battery having an electrolyte solution formed by a mixture of an ether-based aprotic solvent and an ionic liquid

Laura Cecchetto [a], Mark Salomon [b], Bruno Scrosati [a], Fausto Croce [c],*

[a] Department of Chemistry, University of Rome La Sapienza, Piazzale A. Moro, 5-00185 Rome, Italy
[b] MaxPower Inc. 141, Christopher Lane, Harleysville, PA 19438, USA
[c] Dipartimento di Scienze del Farmaco, Università "d'Annunzio" Chieti-Pescara, Via dei Vestini 31, 66100 Chieti, Italy

A B S T R A C T

Recent studies have clearly demonstrated that cyclic and linear carbonates are unstable when used in rechargeable Li–air batteries employing aprotic solvents mostly due to the cathodic formation of superoxide during the oxygen reduction reaction. In particular, it has been ascertained that nucleophilic attack by superoxide anion radical, $O_2^-\bullet$, at O-alkyl carbon is a common mechanism of decomposition of organic carbonates. Moreover, theoretical calculations showed that ether chemical functionalities are stable against nucleophilic substitution induced by superoxide. Aim of this study is to report on a new electrolyte solution for Li–air battery formed by a mixture of an ether-based aprotic solvent with an ionic liquid (IL). The IL-based electrolyte was obtained by mixing the pure ionic liquid N-methyl-(n-butyl) pyrrolidinium bis(trifluoromethane sulfonyl) imide (here denoted as $PYR_{14}TFSI$) to a 0.91 M solution of lithium triflate ($LiCF_3SO_3$) in tetra ethylene glycol dimethyl etcher (TEGDME). We observed that the presence of IL beneficially affects the kinetics and the reversibility of the oxygen reactions involved at the cathode. The most significant result being a lower overvoltage for the charge reaction, compared to a Li/air cell containing the same electrolyte solution without IL.

© 2012 Elsevier B.V. All rights reserved.

1. Introduction

Lithium–air (oxygen) rechargeable batteries utilizing aprotic electrolytes have overcome all other electrochemical battery storage devices in terms of theoretical specific energy [1–9]. Consequently, these batteries have recently drawn considerable attention being an important candidate for energy storage devices for EVs (electric vehicles), HEVs (hybrid electric vehicles) and other high-energy storage applications. However, the practical exploitation of lithium–air systems is still very far due to the numerous scientific challenges that need to be addressed.

The use of a lithium anode combined with an O_2 cathode to obtain a high theoretical energy density was first suggested by Bouman and Littauer [10]. Subsequently Abraham and Jiang [1] demonstrated the utilization of nonaqueous electrolytes in the lithium–air system to avoid the major safety problem of H_2 evolution due to the reaction of lithium with water. The main overall reactions occurring during the discharge process in a lithium–air cell is the reduction of O_2 and oxidation of the metallic lithium to form Li_2O_2 and Li_2O as the reaction products.

Most studies revealed Li_2O_2 as the main reaction product after discharge [1,3], although the formation of Li_2O_2 and Li_2O are both thermodynamically possible since their potentials are quite close. The theoretical potentials for the reactions: (I) $4\,Li + O_2 \rightarrow 2Li_2O$ and (II) $2Li + O_2 \rightarrow Li_2O_2$ are 2.91 and 2.96 V vs. $Li^+/Li°$, respectively, as reported in Refs. [7,11]. Moreover, it has been shown that the nature of the discharge products is mostly controlled by the kinetics of the oxygen reduction which in turn is affected by the presence of a catalyst [3,12], but also by the nature of the electrolyte [13–15]. The main factors limiting the performances of a non-protic Li/air battery are the very high overpotentials for charging (~1 to 1.5 V) compared to the modest overpotentials for discharging (~0.3 V) [1,5]. These overpotentials result in a large system irreversibility, which in turn results in very poor cycleability. At the microscopic level, the processes associated to the charging overpotential have been related to the poor O_2 solubility [3,7] and to the precipitation of the discharge products in the nonaqueous organic electrolytes solutions [16]. In fact, it has been found that insulating discharge products are deposited on the surface of the electrodic active particles, either formed by carbon or by a carbon/catalyst mixture, which block further electron transfer to oxygen and also prevent oxygen from diffusing to the reaction sites [17]. It has also been recently reported in the literature that a key role is played by

---

* Corresponding author. Tel.: +39 0871 3554480; fax: +39 0871 3554483.
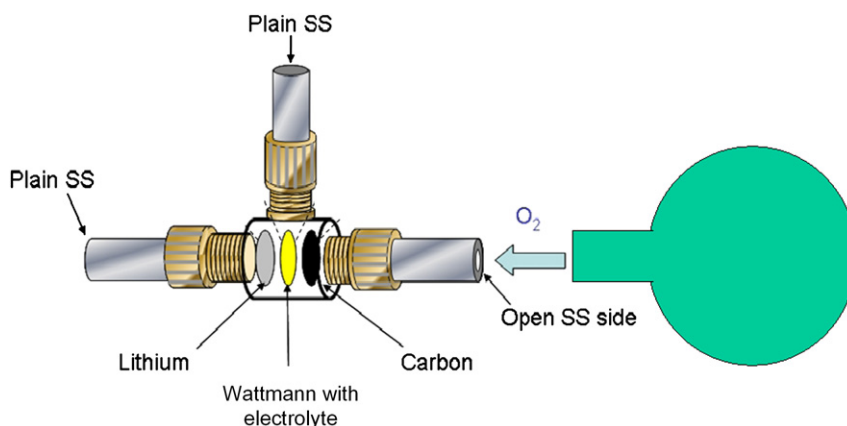 *E-mail address:* fausto.croce@unich.it (F. Croce).

Fig. 1. Li/air cell configuration used for the present study.

the porosity of the cathodic active particles as their pore volume consent the accommodation of the discharge products and their availability for the subsequent charging reaction [17–19]. It follows that acting on the morphology of the cathode supporting material as well as optimising the choice of catalysts for the Oxygen Reduction Reaction (ORR) and for the Oxygen Evolution Reaction (OER) are current important challenges [3,13]. Indeed other important cell parameters, such as the electrolyte composition, could improve the cycle life and the cell efficiency. In fact the electrolyte composition could affect O_2 solubility, but also the nature and the solubility of the discharge reaction products by stabilising intermediary reduction species [21,22] or by binding the oxygen anion in order to overcome the lattice energy of lithium oxides [23].

Recently some important properties of ionic liquids, such as their high conductivity, non-flammability, non-volatility and wide temperature range of operation, have attracted great interest in view of their application as electrolytes in rechargeable Li-ion batteries [24,25]. These same properties could actually be promising for rechargeable Li/air batteries which generally present high overpotentials and poor cycle life as above mentioned. The present manuscript reports preliminary studies concerning the application of an ionic liquid based electrolyte to a lithium/air cell. Pure ionic liquids do not contain mobile Li^+ ions which are necessary for the cell reactions which is the reason why it is necessary to add a lithium salt in order to obtain a lithium-ion conducting electrolyte. To accomplish this, lithium salts having a large, charge-delocalizing anion, are used [24,26]. In our case, the ionic liquid based electrolyte was obtained by mixing the pure ionic liquid N-methyl-(n-butyl) pyrrolidinium bis(trifluoromethane sulfonyl) imide (here noted as $PYR_{14}TFSI$) to a 0.91 M solution of lithium triflate ($LiCF_3SO_3$) in tetraethylene glycol dimethyl ether (TEGDME). The volume ratio between the ionic liquid and the salt solution, in the ionic liquid based electrolyte, was kept 1:1 for all the experiments. Several experiments were also conducted in a Li/air cell containing a 0.91 M solution of lithium triflate ($LiCF_3SO_3$) in tetraethylene glycol dimethyl ether (TEGDME) as the electrolyte solution without the addition of the ionic liquid.

2. Experimental

2.1. Electrodes

Ink slurries for cathode electrodes were prepared by mixing 90% of Super P® carbon black and 10% of PVdF 6020 Solvay Solef® in NMP (Aldrich). The air electrodes were prepared by hand painting the ink onto 10 mm diameter disks of a carbon coated aluminium grid. The electrodes were then dried in air at 150 °C for 24 h and under vacuum at 90 °C over night. The typical carbon loading of the electrodes was of 2–3 mg for each electrode. Anode electrodes were formed by a lithium disk having 10 mm diameter and 0.5 mm thickness.

2.2. Electrolyte solution

A solution of $LiCF_3SO_3$ (Aldrich) in tetraethylene glycol dimethyl ether (TEGDME, Aldrich), was prepared by dissolving 0.91 M of dried $LiCF_3SO_3$ salt in 1 L of TEGDME (hereafter indicated as TEGDME–$LiCF_3SO_3$ electrolyte). The ionic liquid based electrolyte was obtained by mixing the 0.91 M TEGDME–$LiCF_3SO_3$ solution with pure $PYR_{14}TFSI$, provided by Solvionic, in a volume ratio 1:1 (hereafter indicated as $PYR_{14}TFSI$–TEGDME–$LiCF_3SO_3$ electrolyte). Two 300 μm thick, 10 mm diameter Whatman CH disks impregnated with the electrolyte were used to physically separate the anode from the cathode.

2.3. Cell prototypes

The electrodes were assembled in a Swagelok-type three electrode cell formed by a high-density polypropylene body. Fig. 1 reports a schematic of the cell configuration.

The lithium anode foil, the Watman discs and the Super P-based carbon cathode were sandwiched inside the body of the cell with two 10 mm diameter stainless steel plungers acting as current collectors. In this configuration a third lithium reference electrode, provided with its own current collector stainless steel plunger, can be placed in contact with the electrolyte, perpendicularly to the anode/cathode sandwich. The plunger facing the cathode carbon electrode had been bored hollow in order to allow the oxygen that is contained in a latex rubber balloon statically connected to the plunger to reach the electrode/electrolyte interface from the atmosphere. The sealing of the cell is assured by three plastic front ferules.

The electrochemical characteristics of the cell were investigated by Electrochemical Impedance Spectroscopy and Cyclic Voltammetry, both performed with a PAR (Princeton Applied Research) VersaSTAT potentiostat. Impedance data were collected in the frequency range 10^5–1 Hz. Cyclic Voltammetry was performed at a sweep rate of 50 μV s^{-1} in the voltage range 2.2–4 V. The anodic electrochemical stability window of the electrolyte has been determined by performing an anodic scan from the cell open circuit potential to 5.5 V (vs. Li^+/Li) on a Li/electrolyte/Carbon Super P/Al

cell at a scan rate of 200 $\mu V\,s^{-1}$. The ionic conductivity of the electrolyte solution was determined by electrochemical impedance spectroscopy at room temperature in a conductivity cell with two Pt electrodes.

Cell tests were performed at room temperature using a Maccor-4200 battery tester. Charge–discharge curves were recorded galvanostatically at a rate of 25 mA (g carbon)$^{-1}$. We consider here as active material the mass of Super P-carbon in the composite cathode electrode. In the galvanostatic experiment the cell voltage is reported as a function of the specific capacity that is calculated here as the ratio between the amounts of current delivered by (or supplied to) the cell and the mass of active material on the cathode electrode. The cells were first discharged and then charged between the potential limits of 2.2 V (vs. Li$^+$/Li$^\circ$) for discharge and 4.3 V (vs. Li$^+$/Li$^\circ$) for charge.

2.4. XRD measurements

The X-ray diffraction measurements were carried out using a Rigaku instrument equipped with a Cu-Kα source.

3. Results and discussion

The conductivity of the ionic liquid based electrolyte has been measured and compared to the conductivity of a 0.91 M LiCF$_3$SO$_3$ solution in TEGDME at room temperature. The results of such measurements are reported in Table 1.

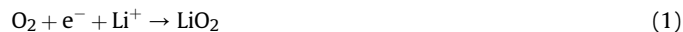As expected the conductivity of the 0.91 M LiCF$_3$SO$_3$ solution in TEGDME greatly improves (4 times) by the addition of the PYR$_{14}$TFSI ionic liquid. This is similar to the significant improvement in conductivity over a very wide temperature range for PYR$_{14}$TFSI mixtures with a quaternary-based liquid electrolyte solution [27].

Fig. 2 reports the electrochemical stability window of the ionic liquid based electrolyte in the absence of oxygen.

It is possible to see that the electrolyte decomposition is observed at potentials higher than 4.8 V (vs. Li$^+$/Li$^\circ$). This suggests that the ionic liquid based solution is stable in the typical potential range used to charge Li/air cell (below 4.5 V vs. Li$^+$/Li$^\circ$) [9]. Fig. 3 shows the cyclic voltammetry traces obtained for the Li/air cell containing the ionic liquid based electrolyte solution.

It is worth to note here that the ionic liquid based electrolyte appears to be stable also in the presence of O$_2$.

According to the results of a recent study [15] the large cathodic peak can be regarded as the result of the overlapping cathodic reactions (1)–(3):

$$O_2 + e^- + Li^+ \rightarrow LiO_2 \tag{1}$$

$$LiO_2 + e^- + Li^+ \rightarrow Li_2O_2 \tag{2}$$

$$Li_2O_2 + 2e^- + 2Li^+ \rightarrow 2Li_2O \tag{3}$$

While the anodic peaks could be attributed to the following oxidation reactions:

Fig. 2. Electrochemical stability window of the ionic liquid based electrolyte in the absence of oxygen.

$$2Li_2O \rightarrow Li_2O_2 + 2e^- + 2Li^+ \tag{4}$$

$$Li_2O_2 \rightarrow LiO_2 + e^- + Li^+ \tag{5}$$

$$LiO_2 \rightarrow O_2 + e^- + Li^+ \tag{6}$$

The onset of the Oxygen Reduction Reaction (ORR) occurs below 2.8 V (vs. Li$^+$/Li$^\circ$) while the Oxygen Evolution Reaction (OER) shows an onset potential at 3.5 V (vs. Li$^+$/Li$^\circ$). Both ORR and OER reactions appear to be quite reversible, at least in the limit of the first six charge–discharge cycles, even if the charge involved in the oxidation process is slightly higher than 100% of the charge involved in the preceding ORR. This finding clearly suggests a certain degree of electrolyte oxidative degradation.

In order to determine the correlation between the electrolyte composition and the overvoltages of both ORR and OER, we performed a galvanostatic cycling test on Li/Air cells whose only difference was the presence of the ionic liquid in the electrolyte solution. The two different cell were cycled with a rate of 25 mA (g carbon)$^{-1}$ and were limited to a specific capacity of 500 mAh g^{-1}.

Fig. 4a and b reports, respectively, the discharge and the discharge–charge voltages vs. the specific capacity of cells with the TEGDME–LiCF$_3$SO$_3$ Electrolyte (black line) or the PYR$_{14}$TFSI–TEGDME–LiCF$_3$SO$_3$ Electrolyte (blue line).

Fig. 4a clearly shows how the discharge occurs for the cells with the two different electrolytes at almost the same voltage 2.6 V (vs. Li$^+$/Li$^\circ$), even if a reproducible slightly higher discharge voltage can be observed for the Li/air cell containing the ionic liquid based solution. The main difference is observed during the charge step; in

Table 1
Conductivity values at 26 °C of the 0.91 M solution of LiCF$_3$SO$_3$ in TEGDME and of the ionic liquid based solution.

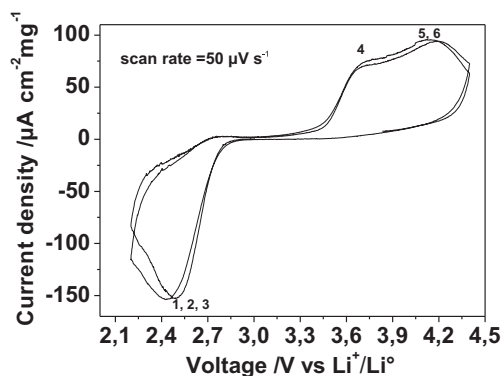| T, °C	TEGDME (LiCF$_3$SO$_3$ 0.91 M), mS cm^{-1}	TEGDME (LiCF$_3$SO$_3$ 0.91 M) + PYR$_{14}$ TFSI, 1:1 volume ratio, mS cm^{-1}
26	0.87	3.5

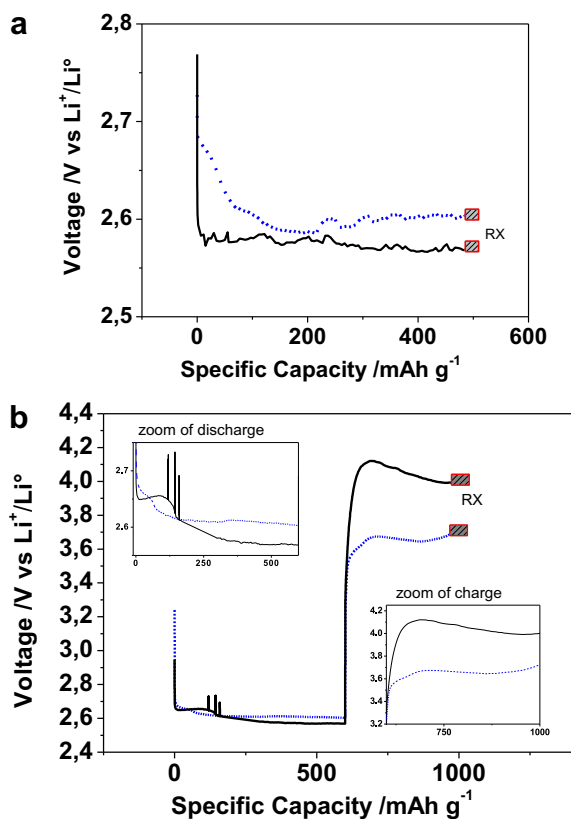**Fig. 3.** Cyclic voltammetry perfomed on a Li/air cell containing the ionic liquid based solution.

Fig. 4. (a) Galvanostatic discharge performed with an applied current of 25 mA g^{-1} on a Li/air cell containing a 0.91 M solution of LiCF$_3$SO$_3$ in TEGDME (black) and a ionic liquid based solution (blue). (b) Galvanostatic discharge−charge performed with an applied current of 25 mA g^{-1} on a Li/air cell containing a 0.91 M solution of LiCF$_3$SO$_3$ in TEGDME (black) and a ionic liquid based solution (blue). (For interpretation of the references to colour in this figure legend, the reader is referred to the web version of this article.)

Fig. 5. (a) XRD pattern of the air cathode of a Li/air cell containing a ionic liquid based solution, performed after discharge (black line) and after charge (red line) at 4.1 V vs. Li+/Li°. (b) XRD pattern of the air cathode on a Li/air cell containing a 0.91 M solution of LiCF$_3$SO$_3$ in TEGDME, performed after discharge (blue line) and after charge (red line) at 3.6 V vs. Li+/Li°. (For interpretation of the references to colour in this figure legend, the reader is referred to the web version of this article.)

fact the overvoltage is significantly reduced, from 4.1 V (vs. Li$^+$/Li°) to 3.6 V (vs. Li$^+$/Li°), in the case of the cell utilizing the ionic liquid added electrolyte. This latter overvoltage value is remarkably low if compared to the values (even considering those at lower rates) reported in the literature [1,11].

In order to better identify the reactions taking place at the air electrode, we have analysed by XRD, for the different electrolytes, the surface composition of the cathode both after a complete galvanostatic discharge and after the following complete charge.

Fig. 5a and b shows the XRD diffraction traces obtained on the cathodes of the Li/Air cells whose galvanostaic cycle numbers are reported in Fig. 4a and b.

From the XRD patterns it is possible to observe that during the charge step the reversible oxidation of Li$_2$O$_2$ occurs; in fact no Li$_2$O$_2$ was be detected by XRD on the electrode surface after this step.

According to these results we can conclude that the addition of the ionic liquid in the electrolyte lowers considerably the overvoltage of the charge process, corresponding to the reversible oxidation of Li$_2$O$_2$, thus suggesting an improved kinetics of the Li$_2$O$_2$ oxidation. This could be reasonably due to a different interface established on the Li$_2$O$_2$ particles that could be thinner or less insulating in the electrolyte containing the ionic liquid. At the same time an improved Li$_2$O$_2$ solubility and thus a smaller particle size could play a role in improving the overvoltage observed during the charge process.

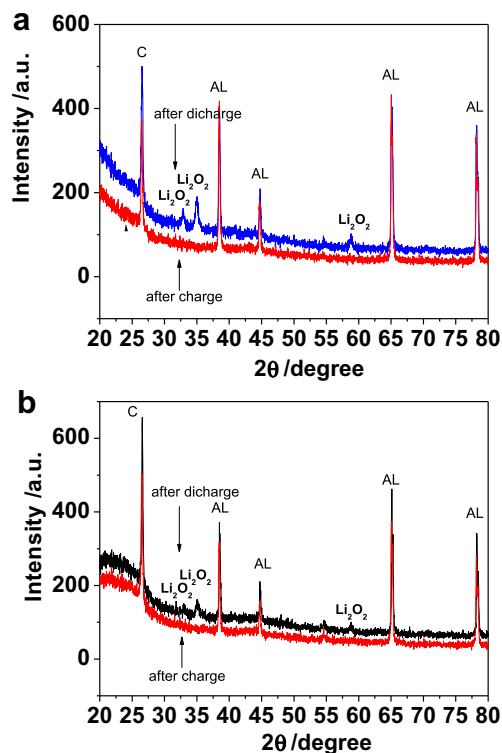Recently it has also been emphasised the influence on the cell behaviour of the ability of the electrolyte in filling the pores of the cathode [16,20]. In fact, if the cathode is only partly wetted by the electrolyte, more free pores are available for the O$_2$ diffusion to the cathode/electrolyte interface. This implies, at the same time, that the surface available for the charge transfer is smaller, the current density is greater and the products of the cell discharge (Li$_2$O$_2$ and, eventually, Li$_2$O) tend to accumulate locally impeding further reactions. We suppose that the lower overvoltage shown by the cell utilizing the ionic liquid added electrolyte is probably due even to better wetting properties of this electrolyte solution that forms a thinner and more uniform liquid layer on the carbon particles which facilitates the O$_2$ diffusion from the free pores to the carbon catalytic sites.

3.1. Electrochemical impedance spectroscopy

To further investigate the cathode/electrolyte interface behaviour during the discharge and the charge process, EIS (Electrochemical Impedance Spectroscopy) measurements have been performed on a pristine air electrode and after repeated discharge/charge cycles.

As shown in Fig. 6 the pristine electrode exhibits a semicircle of small amplitude at high frequencies that suggests the existence of a surface chemical layer at the cathode/electrolyte interface.

The resistance value corresponding to the intercept with the real axis at the highest frequencies investigated can be mainly attributed to the electrolyte bulk resistance and to the resistances at the electrodes/collectors contacts [14,28]. At intermediate frequencies (in the range of hundreds of Hz) it appears a second semicircle of small amplitude, which is overlapped, to the high frequency dispersion. Following the literature [14,29] this semicircle has been associated
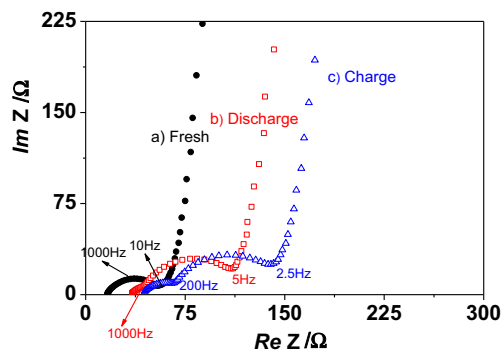
Fig. 6. Impedance spectra of an air electrode in a Li/Air cell containing an ionic liquid based electrolyte: (a) fresh cathode, (b) cathode after discharge and (c) cathode after charge.

Fig. 8. Evolution of the spectra of an air electrode over time in a Li/air cell containing a 0.91 M LiCF$_3$SO$_3$ solution in TEGMDE as electrolyte: (a) fresh cathode, (b) cathode after 1 day and (c) cathode after 2 days. Inset: EIS diagram of the fresh cathode in the Li/air cell containing an ionic liquid based solution (left side) or a 0.91 M LiCF$_3$SO$_3$ solution in TEGDME (right side).

to the charge transfer resistance at the cathode/O$_2$/electrolyte interface. Following the cell discharge, the high frequency semicircle appears almost unchanged, while the amplitude of the intermediate frequency semicircle increases considerably.

This result could be interpreted in terms of Li$_2$O$_2$ formation on the surface of the air electrode after discharge, whose presence could hinder charge transfer and O$_2$ diffusion through the pores of the cathode. However, after recharging the high and the mid frequencies semicircle do not seem to change in a significant way, while, on the other hand, from the diagram it is possible to observe that the intercept with the real axis at high frequencies continuously grows after repeated discharging and charging cycles. The EIS data do not give a clear evidence of a reversible process occurring upon charge, as it would be expected according to the XRD pattern that clearly confirms Li$_2$O$_2$ dissolution. In order to better understand the dynamics of the changes when a fresh air cathode is exposed to the ionic liquid based electrolyte, we studied the EIS of the air cathode at open circuit potential over time. The time evolution of the EIS spectra during ageing is reported in Fig. 7.

The figure shows a continuous evolution of the cathode/air/electrolyte interface. On the fresh electrode the high frequency semicircle and the semicircle at lower frequencies are small and superposed, but they start being clearly distinguished over time. The intercept with the real axis at high frequency continuously grows with time similarly to what observed for the electrode upon discharging and charging. There is a small increase in the amplitude of the small semicircle at high frequency while the amplitude of the second semicircle increases significantly. This result indicates a deep influence on the kinetics of the oxygen reduction reaction by the processes occurring at the electrolyte/air/cathode interface
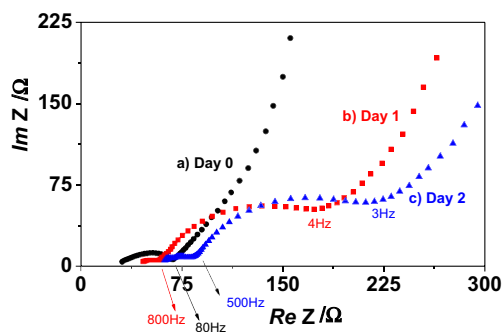
during the first days revealing a dynamic behaviour of the cathode/air/electrolyte interface that could partly mask the effects of Li$_2$O$_2$ formation and dissolution on the EIS spectra.

An in situ chemical analysis would be necessary for a deeper comprehension of the reactions occurring at the carbon/air/electrolyte/ interface, however, the result obtained by the EIS spectra evolution over time could be interpreted in terms of a reaction occurring between the air cathode and the electrolyte with a change of the electrolyte composition or in terms of the build up of a thin solid interface. Both, the change in the electrolyte composition and a growing chemical layer characterised by a small resistive and capacitive behaviour, could justify the improvement of the electrolyte bulk resistance at high frequencies over time. This could also explain a more difficult charge transfer at the cathode/air electrode with ageing.

Fig. 8 reports the evolution of EIS spectra taken over time on the pristine cathode/air electrode in the TEGDME–LiCF$_3$SO$_3$ electrolyte solution.

The shift of the intercept at high frequency is also observed in this case, however, the increase of the charge transfer resistance after two days is much higher. For comparison, the inset of Fig. 8 reports the EIS spectra taken, respectively, on both the pristine cathode/air electrode in the TEGDME–LiCF$_3$SO$_3$ electrolyte and in the PYR$_{14}$TFSI–TEGDME–LiCF$_3$SO$_3$ electrolyte. As expected, according to conductivities, the cathode in the ionic liquid based solution has a lower electrolyte bulk resistance associated with a smaller charge transfer resistance.

These results suggest that the kinetics of oxygen reduction is faster in the LiCF$_3$SO$_3$/TEGDME solution containing the ionic liquid; moreover it seems that the TEGDME/LiCF$_3$SO$_3$ component in the two electrolytes is the main factor responsible for the increase of the charge transfer resistance over time. The different electrolyte composition could affect the nature of the chemical layer and then the kinetics of O$_2$ reduction and oxidation at the cathode/air electrolyte interface.

4. Conclusions

The ionic liquid PYR$_{14}$TFSI has been added to a 0.91 M solution of LiCF$_3$SO$_3$ in TEGDME in a volume ratio 1:1 in order to obtain an ionic liquid based electrolyte for the Li/air batteries.

We observed that the addition of the ionic liquid allows considerably improving the conductivity of the 0.91 M solution of LiCF$_3$SO$_3$ in TEGDME.

Cyclic voltammetry performed on a Li/air cell containing the ionic liquid based electrolyte showed a high degree of reversibility

Fig. 7. Evolution of the spectra of an air electrode in a Li/Air cell containing an ionic liquid based electrolyte over time: (a) fresh cathode, (b) cathode after 1 day and (c) cathode after 2 days.
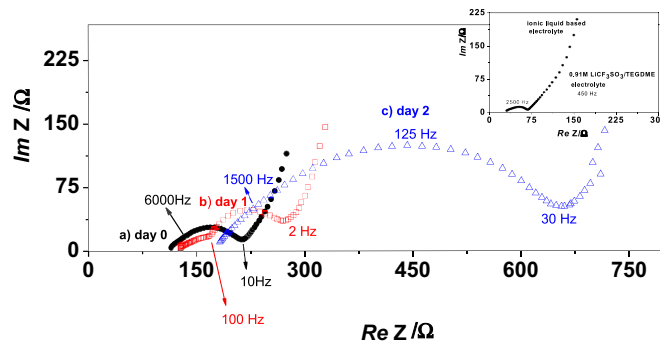
of the reactions involved. Moreover galvanostatic cycling showed a lower overvoltage for the charge reaction, compared to a Li/air cell containing a 0.91 M solution of $LiCF_3SO_3$ in TEGDME. This lower overvoltage could only partly be attributed to the higher conductivity of the ionic liquid based solution.

The XRD analysis performed on the cathode after the charge step confirmed that a reversible oxidation of Li_2O_2 occurred.

EIS data obtained at open circuit potential on pristine cathodes on a Li/Air cell containing a 0.91 M solution of $LiCF_3SO_3$ in TEGDME revealed the presence of a thin solid film at the cathode/air /electrolyte interface whose resistance is lowered when the ionic liquid is present in the electrolyte solution. In addition, EIS measurements also showed that, for the $PYR_{14}TFSI–TEGDME–LiCF_3SO_3$ electrolyte solution, both the bulk resistance and the charge transfer resistance are considerably reduced with respect to Li/air cells operating with the same electrolyte solution without ionic liquid. The effect of the ionic liquid on the charge transfer resistance appears to beneficially affect the kinetics of both the O_2 reduction and oxidation at the cathode air electrode.

According to the results obtained in this paper, this behaviour might partly be attributed to the build-up of a less resistive film at the cathode/air/electrolyte interface on the fresh electrode as well as to an improved Li_2O_2 solubility in the ionic liquid based electrolyte solution, which could lead to a decrease of the Li_2O_2 particle size.

Acknowledgements

References

[1] K.M. Abraham, Z. Jiang, J. Electrochem. Soc. 143 (1996) 1.
[2] J. Read, J. Electrochem. Soc. 149 (2002) A1190–A1195.
[3] A. Débart, A.J. Paterson, J. Bao, P.G. Bruce, Angew. Chem. Int. Ed. 47 (2008) 4521.
[4] T. Kuboki, T. Okuyama, T. Ohsaki, N. Takami, J. Power Sources 146 (2005) 766–769.
[5] T. Ogasawara, A. Débart, M. Holzapfel, P. Novàk, P.G. Bruce, J. Am. Chem. Soc. 128 (2006) 1390–1393.
[6] J. Read, J. Electrochem. Soc. 153 (2006) A96–A100.
[7] Ian Kowalczk, Jeffrey Read, Mark Salomon, Pure Appl. Chem. 79 (2007) 851.
[8] M. Mirzaeian, P.J. Hall, J. Power Syst. Technol. 31 (2007) 90–96.
[9] A. Débart, J. Bao, G. Armstrong, P.G. Bruce, J. Power Sources 195 (2007) 1177.
[10] F. Bauman, E.L. Littauer, Proceedings of the 26th Power Sources Conference, vol. 229 (1978).
[11] Yi-Chun Lu, Hubert A.Gasteiger, Michael C.Parent, Vazrik Chiloyan, Yang Shao-Horn, Electrochem. Solid-State Lett. 13A69 (2010).
[12] Yi-Chun Lu, Hubert A. Gasteiger, Ethan Crumlin, Robert McGuire Jr., Yang Shao-Horn, J. Electrochem. Soc. 157 (2010) A1016.
[13] C. O'Laoire, S. Mukerjee, K.M. Abraham, E.J. Plichta, M.A. Hendrickson, J. Phys. Chem. C 114 (2010) 9178.
[14] C. O'Laoire, S. Mukerjee, E.J. Plichta, M.A. Hendrickson, K.M. Abraham, J. Electrochem. Soc. 158 (2011) A302.
[15] J. Hassoun, F. Croce, M. Armand, B. Scrosati, Angew. Chem. Int. Ed. 50 (2011) 2999–3002.
[16] S.S. Zhang, D. Foster, J. Read, J. Power Sources 195 (2010) 1235.
[17] Chris Tran, Xiao-Qing Yang, Deyang Qu, J. Power Sources 195 (2010) 2057.
[18] S.D. Beattie, D.M. Manolescu, S.L. Blair, J. Electrochem. Soc. 156 (2009) A44.
[19] Jingzhe Chen, Jens S. Hummelshøj, kristian S. Thygesen, Jon S.G. Myrdal, Jens K. Nørskov, Tejs Vegge, Catal. Today 165 (2011) 2.
[20] C.K. Park, S.B. Park, S.Y. Lee, H. Lee, H. Jang, W.I. Cho, Bull. Korean. Chem. Soc. 31 (2010) 3221.
[21] C. O'Laoire, S. Mukerjee, K.M. Abraham, E.J. Plichta, M.A. Hendrickson, J. Phys. Chem. C 113 (2009) 20127.
[22] C. O'Laoire, K.M. Abraham, S. Mukerjee, Electrochem. Soc. Meeting Abstr. 804 (2009) 404 Abstract.
[23] D. Shanmukaraj, S. Grugeon, G. Gachot, S. Laruelle, D. Mathiron, J.-M. Tarascon, M. Armand, J Am. Chem. Soc. 132 (9) (2010) 3055–3062 Mar 10.
[24] A. Fernicola, F. Croce, B. Scrosati, T. Watanabe, H. Ohno, J. Power Sources 174 (2007) 342.
[25] J.H. Shin, E.J. Cairns, J. Power Sources 177 (2008) 537.
[26] M. Kunze, S. Jeong, E. Paillard, M. Winter, S. Passerini, J. Phys. Chem. C 114 (2010) 12364.
[27] D. Bansal, F. Croce, J. Swank, M. Salomon, Conductivities of ionic liquid mixtures with organic electrolyte solutions, in: M. Gaune-Escard, K.R. Seddon (Eds.), Molten Salts and Ionic Liquids: Never the Twain?, John Wiley, Hoboken, 2010.
[28] D. Zhang, R. Li, T. Huang, A. Yu, J.Power Sources 195 (2010) 1202.
[29] Y. Wang, H. Zhou, J.Power Sources 195 (2010) 358.